J Toxicol Pathol 2015; 28: 217–224

Original Article

Application of a compact magnetic resonance imaging system for toxicologic pathology: evaluation of lithium-pilocarpine-induced rat brain lesions

Yoshikazu Taketa[1*], Motohiro Shiotani[1], Yoshiharu Tsuru[2], Sadaharu Kotani[3], Yoshihide Osada[3], Tatsuto Fukushima[3], Akira Inomata[1], and Satoru Hosokawa[1]

[1] Tsukuba Drug Safety, Global Drug Safety, Biopharmaceutical Assessments Core Function Unit, Eisai Product Creation Systems, Eisai Co., Ltd., 5-1-3 Tokodai, Tsukuba, Ibaraki 300-2635, Japan
[2] Research Support Department, Primetech Corp., 1-3-25 Koishikawa, Bunkyo-ku, Tokyo 112-0002, Japan
[3] Neuroscience and General Medicine Product Creation Unit, Eisai Product Creation Systems, Eisai Co., Ltd., 5-1-3 Tokodai, Tsukuba, Ibaraki 300-2635, Japan

Abstract: Magnetic resonance imaging (MRI) is a useful noninvasive tool used to detect lesions in clinical and veterinary medicine. The present study evaluated the suitability of a new easy-to-use compact MRI platform (M2 permanent magnet system, Aspect Imaging, Shoham, Israel) for assisting with preclinical toxicologic pathology examination of lesions in the rat brain. In order to induce brain lesions, male Sprague-Dawley rats were treated once with lithium chloride (127 mg/kg, intraperitoneal [i.p.]) followed by pilocarpine (30 mg/kg, i.p.). One week after dosing, the perfused, fixed brains were collected, analyzed by the MRI system and examined histopathologically. MRI of the brain of treated rats revealed areas of high T1 and middle to low T2 signals, when compared with the controls, in the piriform cortex, lateral thalamic nucleus, posterior paraventricular thalamic nucleus and posterior hypothalamic nucleus of the cerebrum. The altered MRI signal areas were consistent with well-circumscribed foci of neuronal cell degeneration/necrosis accompanied by glial cell proliferation. The present data demonstrated that quick analysis of fixed organs by the MRI system can detect the presence and location of toxicologic lesions and provide useful temporal information for selection of appropriate sections for histopathologic examination before routine slide preparation, especially in complex and functionally heterogeneous organs such as the brain. (DOI: 10.1293/tox.2015-0043; J Toxicol Pathol 2015; 28: 217–224)

Key words: magnetic resonance imaging, pilocarpine, neuronal cell degeneration, rat

Introduction

Magnetic resonance imaging (MRI) is a powerful noninvasive tool used to detect lesions with high sensitivity in clinical medicine[1]. This *in vivo* approach can also be applied to preclinical toxicologic pathology, e.g., for evaluating the time course of a toxic finding and its reversibility in the same animal and for detecting the presence and location of induced lesions, thus assisting with selection of sections for subsequent histopathologic examination. The use of MRI on fixed tissue specimens and perfusion-fixed laboratory animals to make 3-dimensional (3D) digital images has previously been described as magnetic resonance histology (MRH)[2]. This approach is easily applied without prolonged anesthesia and restraint of animals, and it has been examined by several neurotoxicology studies, which demonstrated the usefulness of MRH as a complementary tool for conventional histopathology[3–6]. MRH expands the scope of potential MRI usage and opens up the area for a wider rage of use in preclinical studies. However, barriers to the wide use of MRI systems for preclinical approaches still remain. These include the high cost of purchase and maintenance, significant siting and installation requirements, and complicated operation.

Recently a new compact high-performance MRI platform (M2 permanent magnet system, 1.05 tesla, Aspect Imaging, Shoham, Israel) using a novel magnet design and application-based approach has been developed to reduce the cost and complexity of conventional systems[7]. This system is portable and self-shielded, allowing it to be placed in most research facilities. Cryogens or dedicated supplies are not required. When compared with conventional MRI systems, the advantage of this new system is that it easily provides clear 3D digital morphologic images of an entire

Received: 13 July 2015, Accepted: 7 August 2015
Published online in J-STAGE: 7 September 2015
*Corresponding author: Y Taketa (e-mail: y-taketa@hhc.eisai.co.jp)

target organ. However, this compact MRI has not been sufficiently validated for research purposes.

In MRI analysis, spin-lattice relaxation time (T1) and spin-spin relaxation time (T2) values are frequently encountered, and the normal pattern of these values differs among organs, tissues and fluids[8]. When brain lesions were induced in rats in previous studies, the T1 and T2 signals changed from their normal patterns[9, 10]; these changes in T1- and T2-weighted images allow us to detect induced brain lesions.

Pilocarpine, a muscarinic cholinergic agonist, is a widely accepted agent used to induce status epilepticus and morphologic neuronal damage in the rat brain[11–16]. In this neuronal damage model, clear histologic brain lesions are known to be observed in multiple parts of the cerebrum, such as the piriform cortex, lateral dorsal thalamic nucleus, hippocampus and substantia nigra.

The purpose of the present study was to evaluate the usefulness of this new and easy-to-use compact MRI platform for preclinical toxicologic pathology examination in the pilocarpine-induced rat brain lesion. The changes in T1- and T2-weighted images of the fixed brain were examined by the compact MRI system and compared with histopathologic changes of the neuronal lesions.

Materials and Methods

Animals and husbandry

Six-week-old male Sprague-Dawley (Crl:CD) rats were purchased from Charles River Laboratories Japan, Inc. (Kanagawa, Japan). Animals were maintained at 20–21°C with a relative humidity of 50–60% and a 12-h light/dark cycle. Commercial rodent chow (MF diet, Oriental Yeast Co., Ltd., Tokyo, Japan) and drinking water were available *ad libitum*.

The study protocol was approved by the Laboratory Animal Care and Use Committee and was performed in compliance with the Laboratory Animal Policy of Eisai Co., Ltd.

Chemicals

Lithium chloride (123-01162, Wako Pure Chemical Industries, Osaka, Japan), pilocarpine (161-07201, Wako Pure Chemical Industries) and scopolamine methyl bromide (S8502, Sigma-Aldrich, Tokyo, Japan) were dissolved in 0.9% sodium chloride solution. Diazepam (045-18901, Wako Pure Chemical Industries) was prepared in 1:1:1 (v/v) distilled water, dimethyl sulfoxide and polyethylene glycol 300.

Experimental design

The lithium-pilocarpine model was prepared to induce status epilepticus and brain lesion according to published reports[13]. Sixteen to twenty-four hours before pilocarpine treatment, rats (n = 2) were treated with lithium chloride (127 mg/kg, intraperitoneal [i.p.]). Rats were then injected with scopolamine methyl bromide (5 mg/kg, i.p.) and pilocarpine (30 mg/kg, i.p.). Diazepam (10 mg/kg, intravenous) was administered at 30 min after seizure onset. Control animals (n = 2) were treated with saline, instead of pilocarpine. After 1 week, rats were deeply anesthetized with sodium pentobarbital, flushed with saline and perfused with 4% paraformaldehyde. The fixed brains were removed and submitted for MRI analysis. After the MRI data were obtained, the brains were embedded in paraffin and histopathologically examined.

MRI analysis

High-resolution MRI was performed on fixed brain samples with a compact MRI system (M2 permanent magnet system, 1.05 tesla, Aspect Imaging, Shoham, Israel). Fixed samples were transferred to a modified disposable 10 mL syringe filled with a proton-free susceptibility-matching fluid (Fluorinert FC-77, 3M Company, Saint Paul, MN, USA) and scanned. T1-weighted FLASH-3D sequences were performed under the following parameters: TE (echo time)/TR (repetition time) = 12.0 ms/50.0 ms for about 37 min per sample, 0.10 × 0.10 × 0.48 mm voxel. T2-weighted RARE sequences were performed under the following parameters: TE/TR = 95.0 ms/5484.5 ms for about 8.5 min per sample, 0.15 × 0.15 mm pixel, 1.25 mm slice + 0.25 mm gap. Image processing of the digital 3D MRI data was performed using VivoQuant (inviCRO, Boston, MA, USA), a sophisticated image processing and analysis software package that is fully integrated into the M2 imaging system.

Histopathologic examination

According to a Society of Toxicologic Pathology position paper[17], sections of the forebrain (level 4) and midbrain (level 5) were stained with hematoxylin and eosin (H&E) for histopathologic examination. Histologic changes in the brain were scored according to the following criteria: 1+, neuronal cell degeneration, which was characterized by shrunken and darkened cells with nuclear pyknosis, was sporadically observed without glial cell reaction; 2+, neuronal cell degeneration was diffusely observed and occasionally accompanied by reactive glial cell proliferation; and 3+, widespread neuronal cell necrosis and neuronal loss were present with glial cell proliferation. To visualize the apoptotic cells, terminal deoxynucleotidyl transferase (TdT)-mediated dUTP nick end labeling (TUNEL) staining was performed using an ApopTag Peroxidase *In Situ* Apoptosis Detection Kit (S7100, Chemicon International Inc., Temecula, CA, USA). The deparaffinized sections were incubated with proteinase K (20 µg/ml, S3020, Dako, Tokyo, Japan) for 3 min at room temperature (RT), with 3% hydrogen peroxide for 5 min at RT, with working strength TdT enzyme for 1 hr at 37°C and with Anti-Digoxigenin-Peroxidase for 30 min at RT. The sections were then stained with Liquid DAB+ Substrate Chromogen System (K3468, Dako). Counterstaining was performed with hematoxylin. Sections processed without TdT served as negative controls.

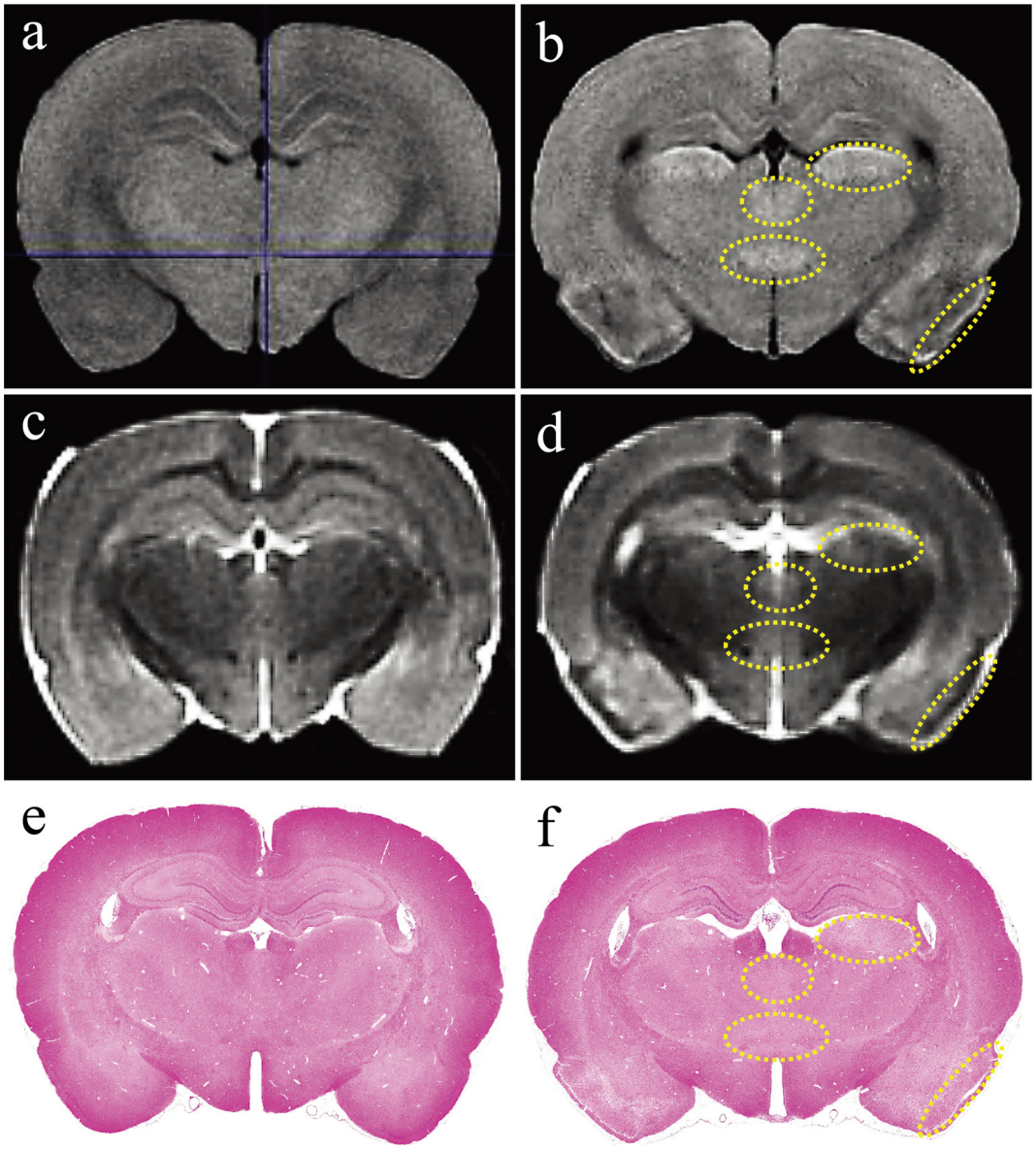

Fig. 1. MRI images (a and b, T1-weighted images; c and d, T2-weighed images) and comparative histology with H&E staining (e and f). The T1-weighted image of the pilocarpine-treated brain (b) showed high T1 signal areas (yellow dotted line regions) compared with control animals (a). In T2-weighted images, the pilocarpine-treated brain (d) showed comparable or low T2 signals compared with the control (c) in the high T1 signal areas. In histology of a comparative cross section with H&E staining, the pilocarpine-treated brain exhibited pale areas in the piriform cortex and lateral thalamic nucleus (f) compared with the control (e).

Results

Clinical observation

Pilocarpine induced continuous, generalized convulsions in rats. Rats were treated with diazepam 30 min after initially achieving severe epileptic behaviors (rearing and falling were considered to indicate as seizure onset). There were no clinical changes in control animals.

MRI analysis

T1- and T2-weighted MRI images and comparative histology are presented in Fig. 1, and a summary of the MRI signal and histopathologic changes in pilocarpine-treated animals is shown in Table 1. The T1-weighted images of the pilocarpine-treated animals showed high T1 signals compared with the controls in the piriform cortex, lateral thalamic nucleus, posterior periventricular thalamic nucleus and posterior hypothalamic nucleus of the cerebrum (Fig. 1a and b). In T2-weighted images of the pilocarpine-treated animals, a low T2 signal compared with the controls were observed in the piriform cortex, which corresponded to a high T1 signal area (Fig. 1c and d). The T2 signal intensities in the other 3 high T1 signal areas were comparable to those of the controls (middle intensity) (Fig. 1c and d). In the his-

Table 1. Summary of MRI Signal and Histopathologic Changes in Pilocarpine-treated Animals

Part of cerebrum	T1 signal	T2 signal	Histopathologic grade
Piriform cortex	↑	↓	3+
Lateral thalamic nucleus	↑	→	2+
Posterior hypothalamic nucleus	↑	→	2+
Posterior paraventricular thalamic nucleus	↑	→	2+
Hippocampus	→	→	2+
Caudate putamen	→	→	1+
Cerebral cortex	→	→	1+
Thalamus	→	→	1+

Histopathologic grades: 1+, sporadical neuronal cell degeneration without glial cell reaction; 2+, diffuse neuronal cell degeneration occasionally accompanied by reactive glial cell proliferation; 3+, widespread neuronal cell necrosis and neuronal loss with glial cell proliferation. n = 2.

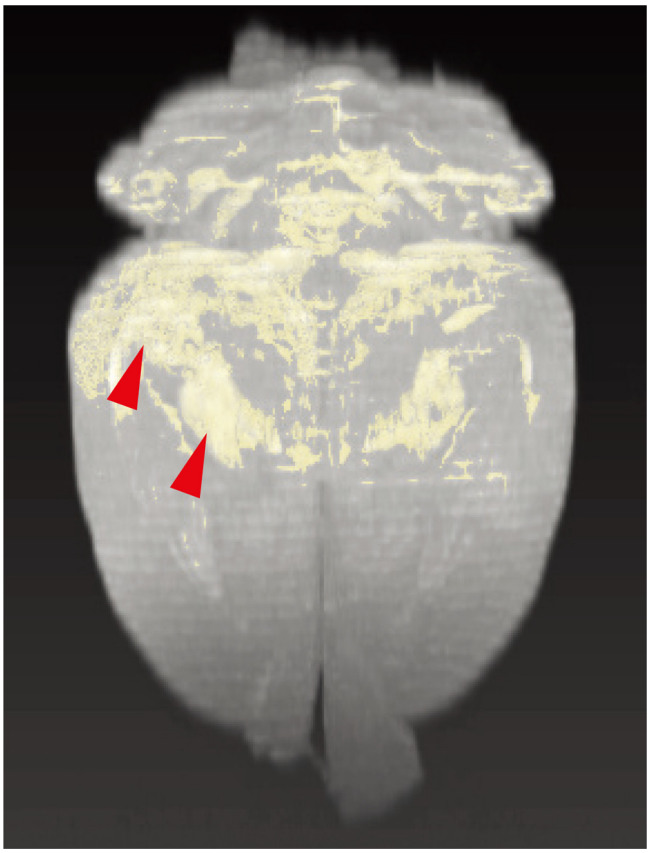

Fig. 2. The 3D T1-weighted MRI image of the pilocarpine-treated brain. Yellowish white areas (arrowheads) correspond to high T1 signals.

tologic examination, brain lesions were clearly identified in the piriform cortex and lateral thalamic nucleus at low magnification as pale areas (Fig. 1e and f). A 3D T1-weighted MRI image of a pilocarpine-treated animal is presented in Fig. 2. In addition to the representative high T1 signal areas in Fig. 1, high T1 signals were also observed in other parts of the brain including the inferior colliculus, visual cortex and flocculus.

Histopathologic changes

Representative histopathologic changes in the midbrain are shown in Fig. 3 and 4. In the 4 high T1 signal areas (piriform cortex, lateral thalamic nucleus, posterior paraventricular thalamic nucleus and posterior hypothalamic nucleus), histopathologic neuronal lesions were observed (Fig. 3). In these areas, diffuse neuronal cell degeneration, which was characterized by shrunken and darkened cells with a pyknotic nucleus, was apparent and was accompanied by widespread necrotic areas, neuronal loss or reactive glial cell proliferation. Additionally, obvious TUNEL-positive apoptotic neuronal cells were observed. Similar changes were confirmed in other cross-sections of high T1 signal areas in the forebrain (data not shown). On the other hand, some areas without clear T1 or T2 signal changes, such as the hippocampus and caudate putamen, showed similar but less expansive neuronal lesions compared with those in high T1 signal areas (Fig. 4). TUNEL-positive cells were also observed in these areas, but there were fewer of them than in high T1 signal areas.

Discussion

The present study demonstrated the suitability of a new compact MRI system for preclinical toxicologic pathology in the lithium-pilocarpine-induced rat brain lesion. Lithium-pilocarpine treatment induced status epilepticus and brain lesion. There were clear correlations between changes in the MRI images and histopathologically detected lesions in the brain.

The lithium-pilocarpine-induced status epilepticus model has been known to induce neuronal lesions in the brain with characteristic distribution in the piriform and entorhinal cortices, thalamus, hippocampus, amygdala, neocortex and substantia nigra[11, 12, 15, 16]. The reported distribution, severity and histopathologic characteristics of the lesions were replicated in the present study.

Since the brain is a functionally and morphologically heterogeneous organ, histopathologic evaluation of neurotoxicity has always been challenging. It is hard to discern the complete distribution pattern of neuronal damage caused by a toxicant when neuropathology is performed on

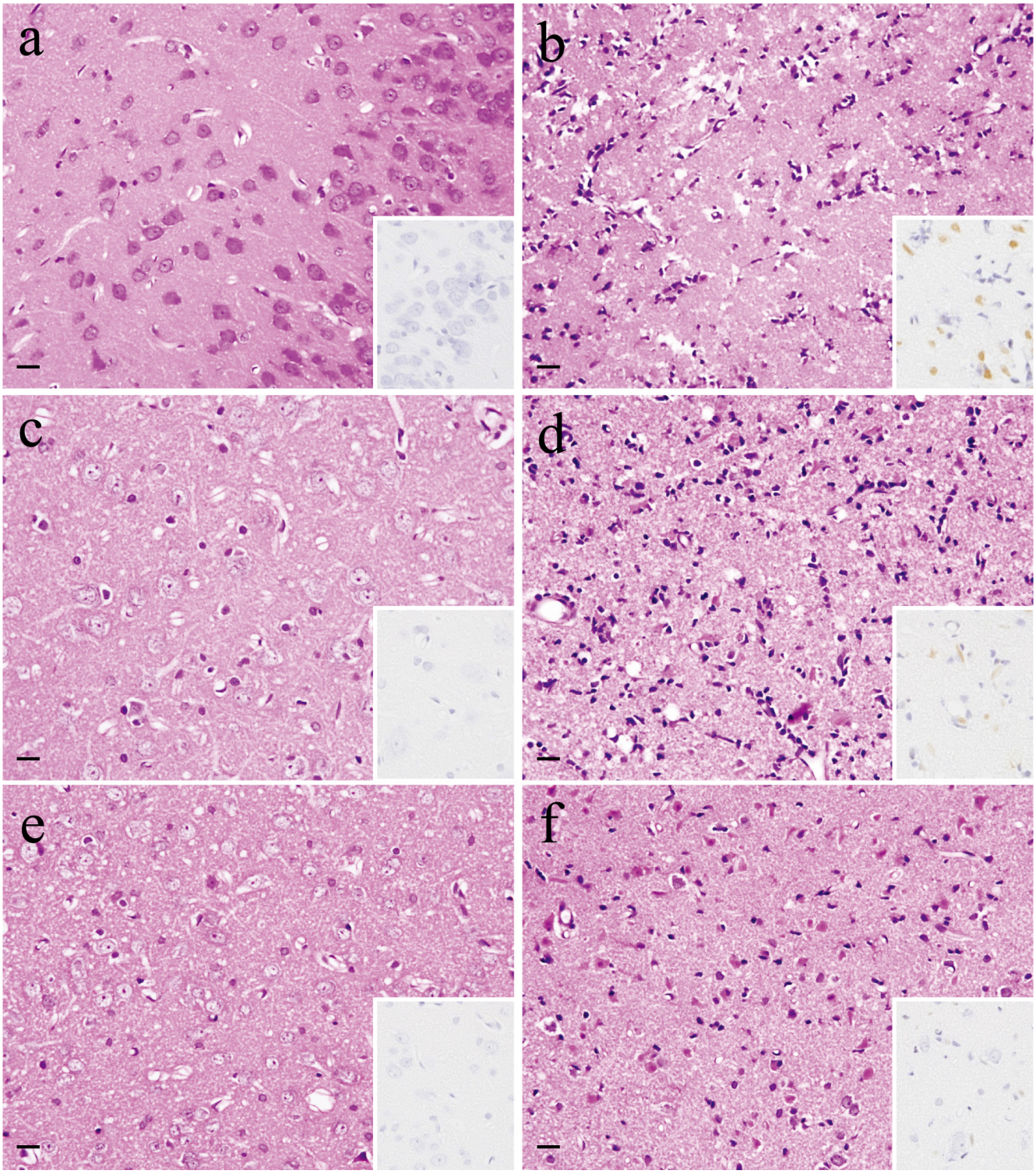

Fig. 3. Cross sections of the piriform cortex (a and b), lateral thalamic nucleus (c and d) and posterior hypothalamic nucleus (e and f) of the cerebrum. The pilocarpine-treated animals showed diffuse neuronal cell degeneration, which was characterized by shrunken and darkened cells with a pyknotic nucleus, accompanied by widespread necrotic areas, neuronal loss or glial cell proliferation with obvious TUNEL-positive apoptotic cells (inset, b, d and f). No histologic changes and no TUNEL-positive cells were observed in the control (a, c and e). Bars = 20 µm.

only a few sagittal or transverse sections. The Society of Toxicologic Pathology recommended the examination of 8 levels of the brain including the cerebrum, midbrain, cerebellum and medulla/pons for neurotoxicity assessment[17], but this requires extra time and resources. The present M2 MRI system efficiently captured clear images of fixed brain, with

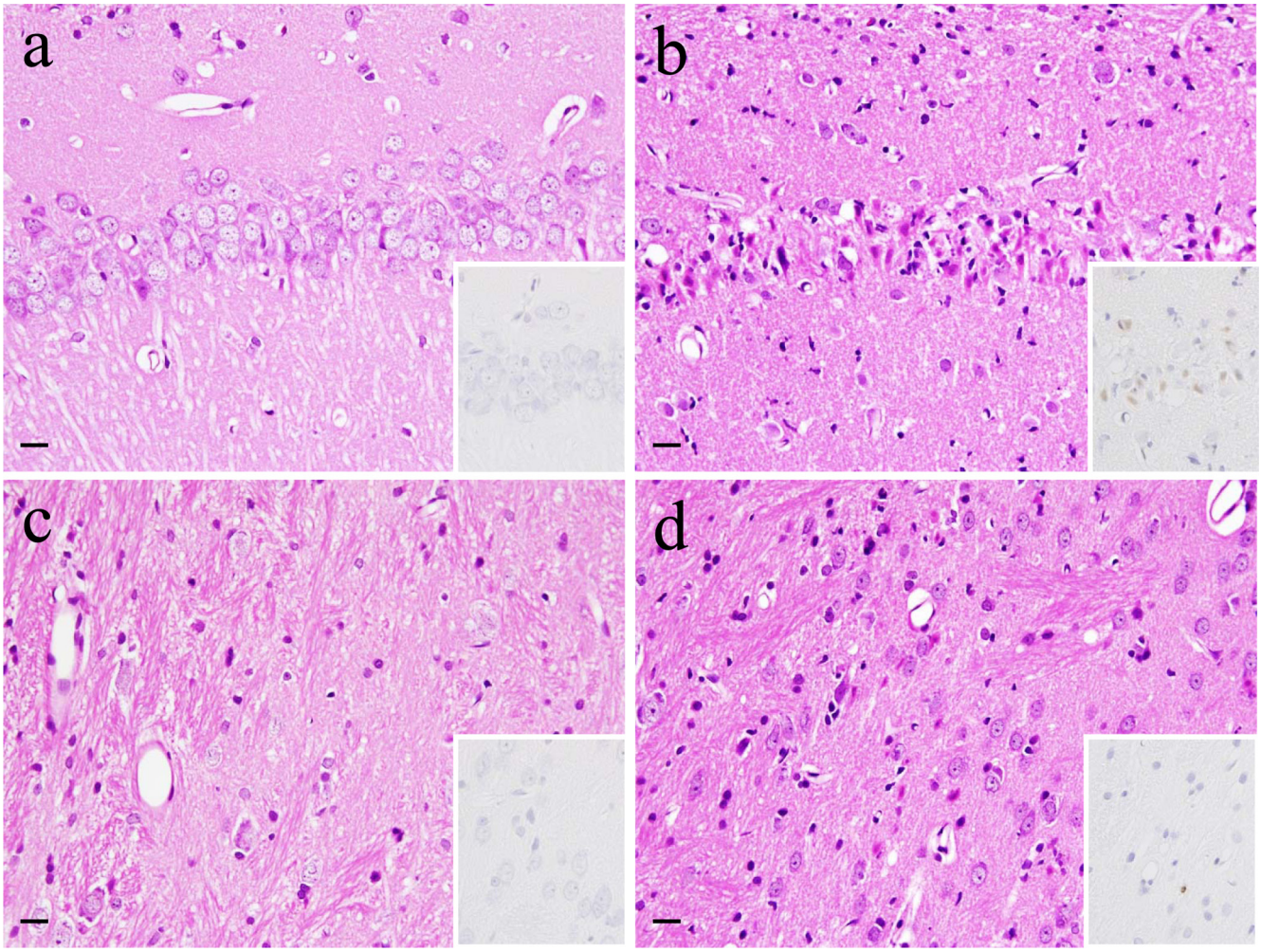

Fig. 4. Cross sections of the hippocampus (a and b) and caudate putamen (c and d). The pilocarpine-treated animals showed neuronal cell degeneration with TUNEL-positive apoptotic cells (inset, b and d). No histologic changes and no TUNEL-positive cells were observed in the control (a and c). Bars = 20 μm.

high enough resolution to reconstruct 3D images, and the automated analyses can be performed. Since the modality is noninvasive and the fixed organ remains intact, traditional histopathology processing and evaluation can be efficiently performed on the same samples following MRI analysis. Therefore, the current compact MRI system can effectively complement traditional neuropathology in routine preclinical toxicity studies.

The present high T1 signal changes had good correlation with histopathologic changes. Considering the T2 signal intensity in the high T1 signal areas, the low T2 signal area in particular showed a severe lesion as a widespread neuronal necrotic area. Fujioka et al. reported that in the ischemic brain lesion in rats, neuronal cell death and gliosis are detected as areas with high T1 and low T2 signals in MRI images[18]. Therefore, the high T1 and low T2 signals in this study are considered to indicate severe neuronal lesions. Meanwhile, T1 and T2 signal intensities were temporally changed in the rat brain ischemic lesion model, with the T1 signal increased from 5 days to 4 weeks after middle cerebral artery occlusion and subsequently decreased until 16 weeks, whereas the T2 signal was increased from 1 to 2 days after middle cerebral artery occlusion and rapidly decreased thereafter[9]. Wegener et al. reported that ischemic necrosis with cystic degeneration leads to a secondary increase in T1 and T2 signals after 2 weeks and that selective neuronal necrosis is accompanied by complete resolution of T1 and T2 signal changes[10]. Therefore, the T1 and T2 signal intensities are considered to change depending on the progress or recovery status of the lesion.

The reason why the selected lesions, such as marked neuronal cell necrosis and glial cell proliferation, showed high T1 and middle to low T2 signals in MRI analysis is a key issue in the present study. Theoretically, the following factors can shorten the T1 and T2 relaxation times: (1) factors immobilizing water molecules, such as a concentrated solution of protein and calcified tissue[19, 20]; (2) lipids[21]; and (3) paramagnetic compounds characterized by having at least 1 unpaired orbital electron including metal ions (e.g., iron, manganese, copper and chromium)[22], molecular oxy-

gen[23] and free radicals[24]. The present high T1 and middle to low T2 signal areas included no histologic hemorrhage or lipid accumulation, and histopathology revealed no clear evidence of protein-rich solution or calcification. However, in the areas with significant neuronal cell necrosis or glial cell proliferation, there might be some changes in the tissue components including the cell population, content of immobilized water molecules or disposition of some neurochemical materials such as paramagnetic species.

Differences in fixation methods may affect the signal intensity and sensitivity of MRI because the water (proton) content of an organ is a key factor in MRI analysis. Formalin fixation does change MRI by decreasing T1 and T2 signals[25, 26]. As a consequence, T1-weighted imaging of the formalin-fixed brain shows a higher signal intensity in gray matter than white matter, the reverse of what is seen *in vivo*[26, 27]. Further investigation into the effect of fixation methods on signal intensity and on sensitivity are required.

In conclusion, the present study proved the suitability of the current easy-to-use compact MRI system in preclinical toxicologic pathology examination of the lithium-pilocarpine-induced rat brain lesion. The high T1 and low T2 signals showed clear histopathologic neuronal lesions although histopathologic examination was more sensitive. The present data demonstrated that quick analysis of fixed organs by the MRI system can detect the presence and location of toxicologic lesions and provide useful temporal information for selection of appropriate sections for histopathologic examination before routine slide preparation, especially in complex and functionally heterogeneous organs such as the brain.

Acknowledgment: We would thank Dr. Kunio Sato, Mr. Masami Kimura, Ms. Michiyo Shimada, Mr. Takaya Shimomura and Mr. Norio Akaogi (Sunplanet Co., Ltd.) for their excellent technical assistance. We also appreciate Ms. Kathy Vanderhoof (Eisai Inc.) for her critical review and helpful comments.

Disclosure of Potential Conflicts of Interest: The authors declare that they have no potential conflicts of interest with respect to the research, authorship, and/or publication of this article.

References

1. Bradley WG. Pathophysiologic correlates of signal alterations. In: Magnetic Sonance in the Central Nervous System. M Brant-Zawadzki (ed). Raven Press, New York. 1986.
2. Johnson GA, Benveniste H, Black RD, Hedlund LW, Maronpot RR, and Smith BR. Histology by magnetic resonance microscopy. Magn Reson Q. **9**: 1–30. 1993. [Medline]
3. Lester DS, Pine PS, Delnomdedieu M, Johannessen JN, and Johnson GA. Virtual neuropathology: three-dimensional visualization of lesions due to toxic insult. Toxicol Pathol. **28**: 100–104. 2000. [Medline] [CrossRef]
4. Maronpot RR, Sills RC, and Johnson GA. Applications of magnetic resonance microscopy. Toxicol Pathol. **32**(Suppl 2): 42–48. 2004. [Medline] [CrossRef]
5. Morgan B, Horsfield MA, and Steward WP. The role of imaging in the clinical development of antiangiogenic agents. Hematol Oncol Clin North Am. **18**: 1183–1206, 2004. [Medline] [CrossRef]
6. Sills RC, Morgan DL, Herr DW, Little PB, George NM, Ton TV, Love NE, Maronpot RR, and Johnson GA. Contribution of magnetic resonance microscopy in the 12-week neurotoxicity evaluation of carbonyl sulfide in Fischer 344 rats. Toxicol Pathol. **32**: 501–510. 2004. [Medline] [CrossRef]
7. Tempel-Brami C, Schiffenbauer YS, Nyska A, Ezov N, Spector I, Abramovitch R, and Maronpot RR. Practical applications of in vivo and ex vivo MRI in toxicologic pathology using a novel high-performance compact MRI system. Toxicol Pathol. **43**: 633–650. 2015. [Medline] [CrossRef]
8. Yokoo T, Bae WC, Hamilton G, Karimi A, Borgstede JP, Bowen BC, Sirlin CB, Chung CB, Crues JV, Bradley WG, and Bydder GM. A quantitative approach to sequence and image weighting. J Comput Assist Tomogr. **34**: 317–331. 2010. [Medline] [CrossRef]
9. Fujioka M, Taoka T, Matsuo Y, Mishima K, Ogoshi K, Kondo Y, Tsuda M, Fujiwara M, Asano T, Sakaki T, Miyasaki A, Park D, and Siesjö BK. Magnetic resonance imaging shows delayed ischemic striatal neurodegeneration. Ann Neurol. **54**: 732–747. 2003. [Medline] [CrossRef]
10. Wegener S, Weber R, Ramos-Cabrer P, Uhlenkueken U, Sprenger C, Wiedermann D, Villringer A, and Hoehn M. Temporal profile of T2-weighted MRI distinguishes between pannecrosis and selective neuronal death after transient focal cerebral ischemia in the rat. J Cereb Blood Flow Metab. **26**: 38–47. 2006. [Medline] [CrossRef]
11. André V, Dubé C, François J, Leroy C, Rigoulot MA, Roch C, Namer IJ, and Nehlig A. Pathogenesis and pharmacology of epilepsy in the lithium-pilocarpine model. Epilepsia. **48**(Suppl 5): 41–47. 2007. [Medline] [CrossRef]
12. Clifford DB, Olney JW, Maniotis A, Collins RC, and Zorumski CF. The functional anatomy and pathology of lithium-pilocarpine and high-dose pilocarpine seizures. Neuroscience. **23**: 953–968. 1987. [Medline] [CrossRef]
13. Hanada T, Ido K, and Kosasa T. Effect of perampanel, a novel AMPA antagonist, on benzodiazepine-resistant status epilepticus in a lithium-pilocarpine rat model. Pharmacol Res Perspect. **2**: e00063. 2014. [Medline] [CrossRef]
14. Löscher W. Animal models of epilepsy for the development of antiepileptogenic and disease-modifying drugs. A comparison of the pharmacology of kindling and post-status epilepticus models of temporal lobe epilepsy. Epilepsy Res. **50**: 105–123. 2002. [Medline] [CrossRef]
15. Persinger MA, Bureau YR, Kostakos M, Peredery O, and Falter H. Behaviors of rats with insidious, multifocal brain damage induced by seizures following single peripheral injections of lithium and pilocarpine. Physiol Behav. **53**: 849–866. 1993. [Medline] [CrossRef]
16. Turski WA, Cavalheiro EA, Schwarz M, Czuczwar SJ, Kleinrok Z, and Turski L. Limbic seizures produced by pilocarpine in rats: behavioural, electroencephalographic and neuropathological study. Behav Brain Res. **9**: 315–335. 1983. [Medline] [CrossRef]
17. Bolon B, Garman R, Jensen K, Krinke G, and Stuart B. Ad Hoc Working Group of the STP Scientific and Regulatory Policy Committee A 'best practices' approach to

neuropathologic assessment in developmental neurotoxicity testing—for today. Toxicol Pathol. **34**: 296–313. 2006. [Medline] [CrossRef]
18. Fujioka M, Taoka T, Matsuo Y, Hiramatsu KI, and Sakaki T. Novel brain ischemic change on MRI. Delayed ischemic hyperintensity on T1-weighted images and selective neuronal death in the caudoputamen of rats after brief focal ischemia. Stroke. **30**: 1043–1046. 1999. [Medline] [CrossRef]
19. Daszkiewicz OK, Hennel JW, and Lubas B. Proton magnetic relaxation and protein hydration. Nature. **200**: 1006–1007. 1963. [CrossRef]
20. Henkelman RM, Watts JF, and Kucharczyk W. High signal intensity in MR images of calcified brain tissue. Radiology. **179**: 199–206. 1991. [Medline] [CrossRef]
21. Fullerton GD. Physiologic basis of magnetic relaxation. In: Magnetic Resonance Imaging. Stark DD and Bradley WG Jr (eds). St Louis, Mosby Year Book. 88–108. 1992.
22. Watson AD, Rocklage SM, and Carvlin MJ. Contrast agents: mechanisms of contrast enhancement. In: Magnetic Resonance Imaging. Stark DD and Bradley WG Jr (eds). St Louis, Mosby Year Book. 374–377. 1992.
23. Weinmann H-J, Gries H, and Speck U. Fundamental physics and chemistry: types of contrast agents. In: MR Imaging of the Skull and Brain: A Correlative Text-Atlas. Sartor K (ed). New York, Springer-Verlag. 26–28. 1992.
24. Haimes AB, Zimmerman RD, Morgello S, Weingarten K, Becker RD, Jennis R, and Deck MDF. MR imaging of brain abscesses. AJR Am J Roentgenol. **152**: 1073–1085. 1989. [Medline] [CrossRef]
25. Kamman RL, Go KG, Stomp GP, Hulstaert CE, and Berendsen HJC. Changes of relaxation times T1 and T2 in rat tissues after biopsy and fixation. Magn Reson Imaging. **3**: 245–250. 1985. [Medline] [CrossRef]
26. Nagara H, Inoue T, Koga T, Kitaguchi T, Tateishi J, and Goto I. Formalin fixed brains are useful for magnetic resonance imaging (MRI) study. J Neurol Sci. **81**: 67–77. 1987. [Medline] [CrossRef]
27. Unger EC, Gado MH, Fulling KF, and Littlefield JL. Acute cerebral infarction in monkeys: an experimental study using MR imaging. Radiology. **162**: 789–795. 1987. [Medline] [CrossRef]